Local symmetry lowering in the cubic intermetallics YbPdBi and YbNiSb

1995 J. Phys.: Condens. Matter 7 5665

(http://iopscience.iop.org/0953-8984/7/28/020)

J. Phys.: Condens. Matter 7 (1995) 5665–5680. Printed in the UK

Local symmetry lowering in the cubic intermetallics YbPdBi and YbNiSb

G LeBras†, P Bonville†, J A Hodges†, J Hammann†, M J Besnus‡, G Schmerber‡, S K Dhar§, F G Aliev‖ and G André¶

† CEA, CE Saclay, DRECAM/SPEC, 91191 Gif-sur-Yvette, France
‡ IPCMS, 23 rue du Loess, 67037 Strasbourg, France
§ Tata Institute of Fundamental Research, Homi Bhabba Road, Bombay 400005, India
‖ Moscow State University, Physics Department, 119899 Moscow, Russia
¶ Laboratoire Léon Brillouin, CE Saclay, 91191 Gif-sur-Yvette, France

Received 22 February 1995, in final form 19 April 1995

Abstract. A microscopic investigation of the cubic ternary alloys YbPdBi and YbNiSb, using ^{170}Yb Mössbauer spectroscopy, reveals that the point symmetry at the site of the Yb^{3+} ion is far from cubic in both compounds. An analysis of the thermal variation of the quadrupolar 4f moment shows that the energy of the first crystal electric field transition is close to 20 K in YbPdBi and to 10 K in YbNiSb. Specific heat measurements are also presented in YbPdBi, and magnetic ordering is detected below 1 K in YbPdBi, with saturated Yb^{3+} moments of 1.25 μ_B, and below 0.85 K in YbNiSb, with saturated moments of 1 μ_B. A tentative explanation of the Yb site symmetry breaking is made in terms of a Jahn–Teller distortion within the Γ_8 cubic quartet.

1. Introduction

Among the ternary Yb intermetallics crystallizing into the cubic MgAgAs-type structure (f.c.c. lattice, $F\bar{4}3m$ space group), unusual low-temperature properties have been evidenced in YbPdSb and YbPtBi. The compound YbPdSb is a Kondo lattice very close to the magnetic–non-magnetic transition, where the ground crystal electric field state of the Yb^{3+} ion is the Γ_8 quartet [1–4]; in the compound YbPtBi, a phase transition occurs at 0.4 K, and the ground state is thought to consist of paramagnetic regions and magnetically ordered regions, with small Yb^{3+} magnetic moments, in roughly equal proportions [5–7].

We present here a ^{170}Yb Mössbauer spectroscopy investigation of two other members of this series, YbPdBi and YbNiSb, in the temperature range 0.1 K–50 K, and specific heat measurements in YbPdBi in the temperature range 0.5 K–45 K. An x-ray diffraction spectrum at 20 K, and neutron diffraction spectra at 130 K and 1.5 K, have also been performed for YbPdBi. Previous short studies of the specific heat [8] and the transport properties [9] in YbPdBi suggested the presence of the Kondo effect, and of heavy-electron behaviour; a recent specific heat work on YbNiSb [10] evidences a magnetic transition at 0.85 K. Our present investigation, down to very low temperature (0.1 K), shows the presence of a magnetic phase transition in YbPdBi at $T_N \simeq 1$ K, and confirms the magnetic transition in YbNiSb. The thermal variation of the Yb^{3+} spontaneous magnetic moment has been measured in both compounds. Furthermore, due to the local character of the Mössbauer probe, our study reveals the rather unexpected fact that the symmetry of the Yb

0953-8984/95/285665+16$19.50

site is not cubic either in YbPdBi or in YbNiSb. The thermal variation of the 4f quadrupolar moment of the Yb^{3+} ion, measured *via* the quadrupolar hyperfine interaction at the ^{170}Yb nucleus, allows us to detect the presence of a low-lying crystal electric field (CEF) Kramers doublet in both compounds. These low-energy CEF states (1–2 meV) are not easily resolved in the inelastic neutron scattering spectra of intermetallic compounds, because of the large broadening of the quasielastic line, even at low temperature.

This paper is organized as follows: section 2 contains the experimental details, sections 3 and 4 describe the experimental data respectively in YbPdBi and YbNiSb, and section 5 contains the interpretation and a discussion about the crystal electric field level scheme of the Yb^{3+} ion and the origin of the local symmetry breaking.

2. Experimental set-up

The Mössbauer transition of the ^{170}Yb isotope has an energy E_0 of 84.3 keV and links the ground nuclear state, with spin $I_g = 0$, to the first excited nuclear state, with spin $I = 2$. The velocity unit 1 mm s^{-1} corresponds, for ^{170}Yb, to an energy of 68 MHz ($E = E_0 v/c$). The γ-ray source is neutron-activated Tm^*B_{12}, which yields a single Lorentzian line with width (FWHM) 2.8 mm s^{-1}, with a reference $YbAl_3$ absorber. The spectra were recorded using a triangular velocity electromagnetic drive.

The specific heat measurements were performed using the adiabatic calorimetry method, and the magnetic susceptibility measurements using a standard extraction technique.

The neutron diffraction spectra in YbPdBi were obtained on the powder diffractometer G4.1, equipped with a 800-cell multidetector, installed at the Orphée reactor at the LLB.

The samples are polycrystalline; the YbPdBi sample has been prepared by melting the constituents in stoichiometric proportions in an arc furnace, with subsequent annealing, and the YbNiSb sample has been prepared by repeated meltings in a closed crucible in an induction furnace [11].

3. The experimental results in YbPdBi

3.1. X-ray and magnetic susceptibility characterization

The powder x-ray diffractogram of our sample shows the lines of the YbPdBi f.c.c. lattice, with lattice parameter at room temperature $a = 6.5975(5)$ Å, and three lines of an unidentified impurity phase, with ~10% relative weight. The line intensities in the YbPdBi phase spectrum are only compatible with an atomic basis having Pd in (0, 0, 0), Yb and Bi occupying the two other sites of the MgAgAs-type stucture: $(\frac{1}{4}, \frac{1}{4}, \frac{1}{4})$ and $(-\frac{1}{4}, -\frac{1}{4}, -\frac{1}{4})$. As the diffusion factors for Yb and Bi are not very different, the line intensities are not sensitive to an eventual crystallographic disorder involving Yb and Bi.

The magnetic susceptibility is characteristic of the presence of Yb^{3+} ions, with antiferromagnetic exchange interactions; it follows a Curie–Weiss law down to 15 K:

$$\chi(T) = \frac{\mu_{eff}^2}{3k_B(T + \Theta_p)} \tag{1}$$

with $\mu_{eff} \simeq 4.2\ \mu_B$ and $\Theta_p \simeq 6$ K. The raw effective moment of 4.2 μ_B is somewhat smaller than the free-ion moment 4.54 μ_B. Taking into account the presence of 10% impurity phase, and assuming that it does not contain Yb^{3+} ions, one gets a corrected effective moment per Yb^{3+} ion of 4.4 μ_B, closer to the expected free-ion value.

3.2. Specific heat

Specific heat data were obtained in YbPdBi (figure 1) and in LuPdBi, taken as the non-magnetic reference. In this latter compound, the specific heat $C(T)$ increases monotonically with increasing temperature, and, below 5 K, follows the law

$$C = \gamma T + \beta T^3 \tag{2}$$

with $\gamma = 1.09$ mJ K^{-2} mol^{-1} and $\beta = 0.64$ mJ K^{-4} mol^{-1}. With the assumption that the electronic band and phonon contribution to the YbPdBi specific heat is well represented by the LuPdBi specific heat, the 4f contribution in YbPdBi can be obtained by subtraction, and is represented in figure 2. The dashed line in this figure is the CEF Schottky anomaly, with the first excited CEF doublet at an energy 23 K, as discussed in section 5.1. The peak at 1 K (inset to figure 1) corresponds to a magnetic ordering transition, as will be confirmed by the Mössbauer study (see section 3.4). As often observed in Yb intermetallic compounds, the transition is spread over a few 0.1 K, probably because of the presence of a distribution of transition temperatures in the crystallites. The peak value $C_{4f}(1\text{ K}) = 3.1$ J K^{-1} mol^{-1} is much smaller than expected for a second-order transition for an electronic Kramers doublet (12.4 J K^{-1} mol^{-1}). The entropy released by the magnetic transition, estimated by assuming that $C_{4f}/T|_{T\to 0}$ is worth 0.5 or 1 J K^{-2} mol^{-1}, amounts to $\simeq 0.4R\ln 2$ at 1.3 K, which is much smaller than the value $R\ln 2$, expected for a doublet ground state. The entropy gain reaches $R\ln 2$ at $T = 5$ K. The 4f-derived specific heat remains at the constant value 2.2 J K^{-1} mol^{-1} between 1.3 K and 3 K, then rises rapidly to reach 5.1 J K^{-1} mol^{-1} at about 10 K, and varies slowly at higher temperature, outlining a faint maximum near 25 K. The associated entropy gain reaches $2.75R\ln 2$ at 45 K, the overall entropy variation of the ground $\{J = \frac{7}{2}\}$ spin–orbit multiplet of the Yb^{3+} ion being $R\ln 8$.

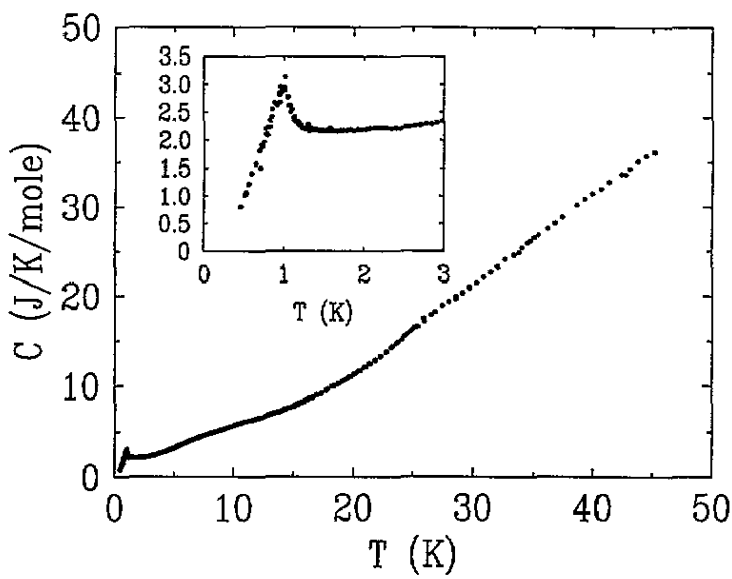

Figure 1. Thermal variation of the specific heat in YbPdBi; inset: low-temperature magnetic transition anomaly.

The $\gamma(T) = C_{4f}(T)/T$ ratio (inset to figure 2) increases monotonically with decreasing temperature: from 0.5 J K^{-2} mol^{-1} at 10 K, it reaches 0.7 J K^{-2} mol^{-1} at 3 K, then increases steeply down to the magnetic transition temperature. The dashed lines in figure 2

correspond to the assessed CEF Schottky anomaly (see section 5.1). The rapid rise of the 4f specific heat between 3 K and 10 K occurs thus with an almost constant γ value of 0.5–0.7 J K^{-2} mol^{-1}; between 5 K and 10 K, the main contribution to this high γ value comes from the Schottky anomaly. From these data, it is therefore difficult to derive a value for the low-temperature electronic γ coefficient that would reflect the presence of Kondo or heavy-electron behaviour (see also the discussion in section 5.3).

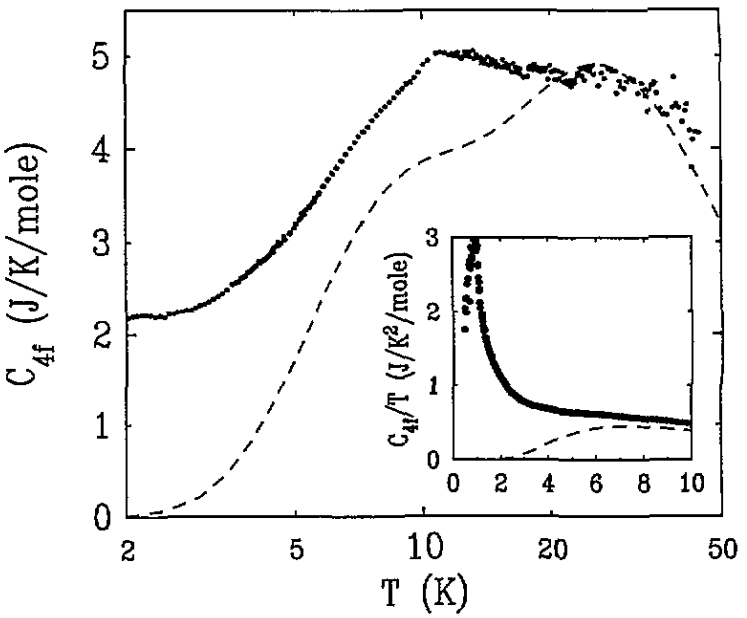

Figure 2. Thermal variation of the electronic 4f specific heat in YbPdBi; inset: thermal variation of the C_{4f}/T ratio. The dashed lines represent the calculated Schottky anomaly (see text).

3.3. ^{170}Yb Mössbauer spectroscopy data in the paramagnetic phase ($T > 1$ K)

The ^{170}Yb Mössbauer absorption spectra above 1 K show a rather symmetrical resolved three-line structure up to 10 K (see the $T = 4.2$ K spectrum in figure 3), with relative line intensities close to the ratio 2:1:2, and an overall splitting which smoothly decreases as temperature increases. At higher temperature, the spectra become less resolved (see the $T = 13$ K spectrum in figure 3) and, above 20 K, consist of a broad line whose width rapidly decreases as temperature increases. The surprising feature is that the low-temperature spectra are not one-line spectra, expected for a Yb^{3+} ion in cubic symmetry, hence with zero quadrupolar hyperfine interaction. However, as the intensity ratio and the line splitting are characteristic of ^{170}Yb quadrupolar hyperfine interactions, we interpret these spectra as due to the presence of a non-zero electric field gradient (EFG) tensor V_{ij} at the Yb site, with main components such that $V_{ZZ} \simeq -V_{XX}$, and $V_{YY} \simeq 0$, i.e. an asymmetry parameter $\eta = (V_{XX} - V_{YY})/V_{ZZ}$ close to unity. Further arguments supporting this interpretation will be given in section 3.5. The evidence for a non-zero quadrupolar interaction in the paramagnetic phase of YbPdBi implies that the Yb site symmetry is not cubic in this compound.

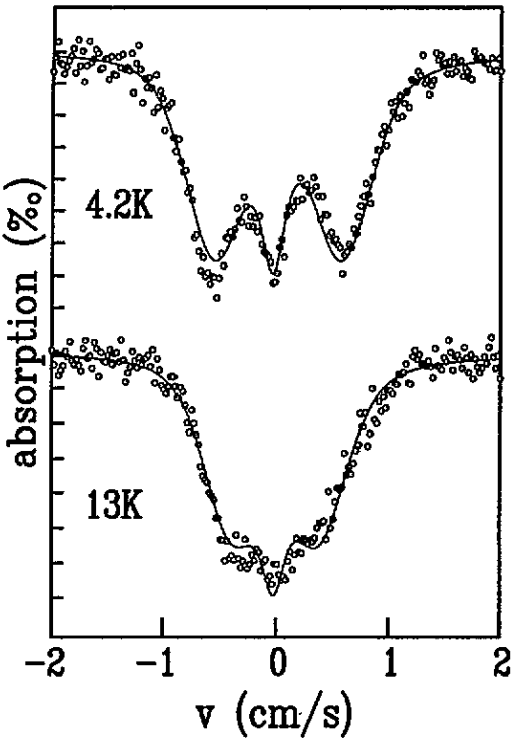

Figure 3. ^{170}Yb Mössbauer absorption spectra in YbPdBi in zero field at 4.2 K and 13 K. The continuous lines are fits to Hamiltonian (3) with a Gaussian distribution of quadrupolar coupling parameter values.

The spectra can be fitted to the quadrupolar hyperfine Hamiltonian

$$\mathcal{H}_Q = \alpha_Q \left[I_Z^2 - \frac{I(I+1)}{3} + \frac{\eta}{6}(I_+^2 + I_-^2) \right] \tag{3}$$

where $\alpha_Q = (eQV_{ZZ})/8$ is the quadrupolar coupling parameter, proportional to the Z component V_{ZZ} of the EFG tensor, and Q is the electric quadrupole moment of the excited nuclear state of spin I. The linewidths are somewhat inhomogeneous and rather large, which we interpret as a static broadening due to the presence of a distribution of EFG component values at the Yb site (see section 3.5). The continuous lines in figure 3 are fits to Gaussian distributions of α_Q values, with centre α_Q^0 and mean square deviation $\sigma(\alpha_Q)$. The obtained parameter values are: at $T = 4.2$ K, $\alpha_Q^0 = 2.77(5)$ mm s^{-1}, $\sigma(\alpha_Q) = 0.86$ mm s^{-1} and $\eta = 0.89$; at $T = 13$ K, $\alpha_Q^0 = 1.87(5)$ mm s^{-1}, $\sigma(\alpha_Q) = 0.83$ mm s^{-1} and $\eta = 0.95$. The thermal variation of α_Q^0 is represented in figure 4. Below 5 K, it shows a saturated value corresponding to the EFG created by the intrinsic 4f quadrupolar tensor of the ground Yb^{3+} doublet, which is non-zero at a non-cubic site, to which must be added a smaller (unknown) lattice EFG contribution. The rapid decrease of α_Q^0 as temperature increases above 10 K points to the presence of a low-lying excited crystal electric field doublet. The asymmetry parameter η shows very little thermal variation.

3.4. ^{170}Yb Mössbauer data in the magnetically ordered phase ($T < 1$ K)

At $T = 0.035$ K, the ^{170}Yb Mössbauer absorption spectrum, represented in figure 5, consists of five lines, the most energetic line being strongly broadened. It corresponds to the presence of a magnetic hyperfine interaction superposed onto the quadrupolar hyperfine interaction

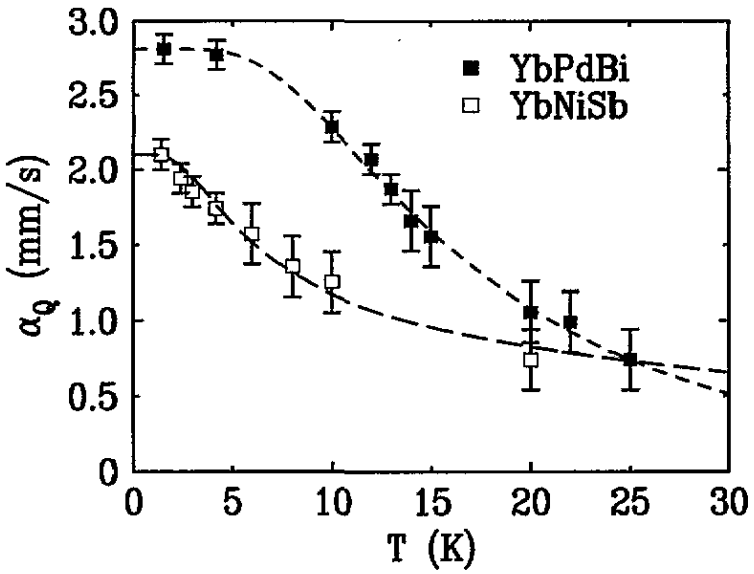

Figure 4. Thermal variation of the mean Mössbauer-derived quadrupolar parameter α_Q^0 in YbPdBi (black squares) and YbNiSb (open squares); the dashed lines represent calculated thermal variations with CEF level schemes described in the text.

evidenced in the paramagnetic phase, described by the Hamiltonian

$$\mathcal{H} = -g_n \mu_n \boldsymbol{I} \cdot \boldsymbol{H}_{hf} + \mathcal{H}_Q \tag{4}$$

where g_n is the nuclear excited state gyromagnetic ratio and $\boldsymbol{H}_{hf}$ the hyperfine field at the nucleus. The hyperfine field, which for rare earths is proportional, to a good approximation, to the spontaneous electronic moment (H_{hf} (T) = $102m$ (μ_B) for $^{170}Yb^{3+}$), indicates the presence of magnetic ordering of the Yb^{3+} moments. In order to fit this spectrum, as well as those at higher temperature, the hyperfine quadrupolar parameters α_Q and η were kept at their saturated values obtained in the paramagnetic phase, a procedure which is valid if the exchange interaction (the magnetic ordering temperature) is much lower than the energy of the first CEF excited doublet. In such a case, the exchange field present in the magnetically ordered phase induces a small mixing of the excited doublet into the ground doublet, resulting in a small variation of the 4f quadrupolar tensor, and hence of the EFG tensor. In YbPdBi, the exchange interaction ($T_N \simeq 1$ K) is much smaller than the first CEF excitation ($\simeq 20$ K, see section 5.1) and the EFG tensor below T_N is not expected to be essentially different from its saturated paramagnetic value.

The saturated hyperfine field value at 0.035 K fitted to Hamiltonian (4) is H_{hf} = 127.5(10) T, corresponding to a saturated spontaneous electronic moment $m = 1.25(10)\ \mu_B$. The direction of the hyperfine field (i.e. of the magnetic moment) is determined by the crystalline anisotropy (g tensor) and by the anisotropy (if any) of the exchange interaction. The directions of the principal axes $OXYZ$ of the EFG tensor are determined by the local symmetry at the Yb site and, at a site with low symmetry, there is no reason why they should coincide with the magnetic anisotropy axes. Therefore, the orientation of $\boldsymbol{H}_{hf}$ with respect to the $OXYZ$ axes has to be introduced, and the best fit yields θ (polar angle) $\simeq 40°$ and γ (azimuthal angle) $< 20°$. However, as the orientation of the $OXYZ$ axes with respect to the crystal axes is not known, the direction of $\boldsymbol{H}_{hf}$ and hence of $\boldsymbol{m}$ cannot be determined.

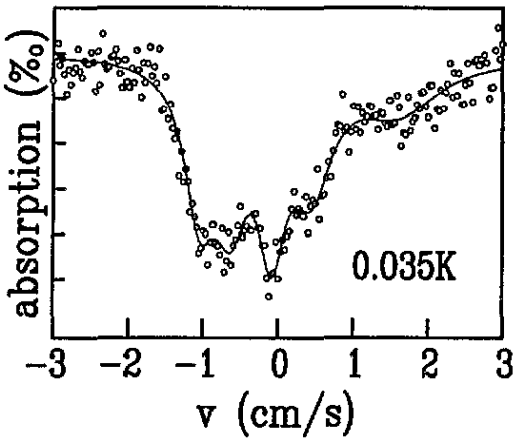

Figure 5. ^{170}Yb Mössbauer absorption spectrum in YbPdBi in zero field at $T = 0.035$ K. The continuous line is a fit to Hamiltonian (4) with Lorentzian lines having different linewidths.

The very inhomogeneous linewidths of the $T = 0.035$ K spectrum are of static origin, as no dynamical broadening can occur at such low temperature. They are the hallmark of correlated distributions of hyperfine fields H_{hf} and quadrupolar parameters α_Q, arising from a distribution of small crystal field distortions at the Yb site [12]. These distortions give rise to a distribution of CEF energies and eigenfunctions and, in the case where the root mean square deviation of the CEF energy distribution is small with respect to the CEF level splitting, a perturbation calculation yields a linear correlation between the H_{hf} and α_Q values. The $T = 0.035$ K spectrum can be satisfactorily fitted with linearly correlated Gaussian distributions of H_{hf} and α_Q parameters, with mean values $H^0_{hf} = 130$ T and $\alpha^0_Q = 2.9$ mm s^{-1}, and root mean square deviations $\sigma(H_{hf}) = 59$ T and $\sigma(\alpha_Q) = 0.5$ mm s^{-1}. These relatively high values show that the root mean square deviation of the distribution of CEF energies $\sigma(E)$ must be of the order of a few K; the estimation of the CEF splittings in YbPdBi (see section 5.1) confirms that $\sigma(E)$ is much smaller than the energy of the first CEF excited state.

As temperature increases, the fitted hyperfine field decreases and the magnetic hyperfine structure collapses; the paramagnetic three-line spectrum is recovered at 1 K. The thermal variation of the mean spontaneous Yb^{3+} magnetic moment derived from the hyperfine field values is shown in figure 6. It approximately follows a mean-field law for $S = \frac{1}{2}$, expected for a Kramers doublet ground state, with a transition temperature $T_N \simeq 0.85(5)$ K. The Mössbauer-derived transition temperature is slightly smaller than the temperature for which the specific heat shows a peak (1 K). The Mössbauer spectrum at 1 K presents, however, a broadened most energetic line, which could be due to the presence of short-range ordering a few 0.1 K above T_N, as suggested by the tail of the specific heat peak (see inset of figure 1).

3.5. Static against dynamic interpretation of the Mössbauer spectra

The occurrence of a split spectrum in the paramagnetic phase of a cubic compound raises the question of the magnitude of the Yb^{3+} fluctuation rate ν with respect to the magnetic hyperfine frequencies ν_{hf}. Indeed, in the so-called 'slow- or intermediate-relaxation' regime, i.e. for $\nu \ll \nu_{hf}$ or $\nu \sim \nu_{hf}$, resolved paramagnetic hyperfine spectra are observed in the paramagnetic phase in cubic symmetry. However, the thermal evolution of such spectra as well as the magnitude of the spectral splittings is specific and very different from what is observed in YbPdBi and YbNiSb (see section 4 for the latter compound). The spectral splittings in an 'intermediate-relaxation' spectrum are of the order of magnitude of

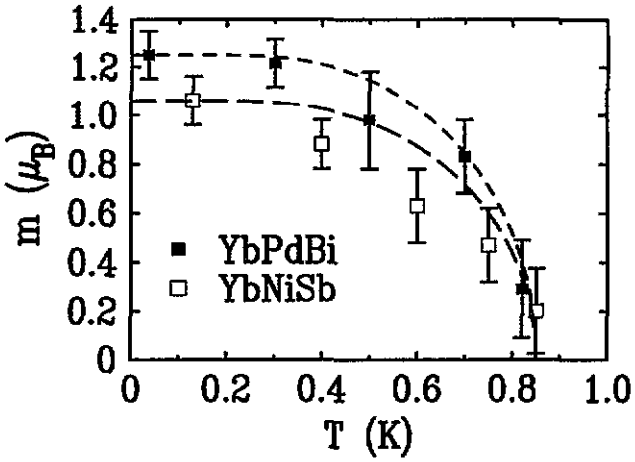

Figure 6. Thermal variation of the spontaneous Yb^{3+} electronic moment in YbPdBi (black squares) and YbNiSb (open squares), derived from the hyperfine field values. The dashed lines are $S = \frac{1}{2}$ mean-field curves with $T_N = 0.85$ K for both compounds.

the magnetic hyperfine interaction, i.e. 30–60 mm s^{-1} for ^{170}Yb, whereas the maximum overall splitting observed is 11 mm s^{-1} in YbPdBi and 8 mm s^{-1} in YbNiSb, typical of the quadrupolar hyperfine interaction. As temperature increases, i.e. as relaxation speeds up, the lines of an 'intermediate-relaxation' spectrum do not change position and acquire appreciable dynamical broadenings, which usually results in the fact that no anomaly is observed at the magnetic transition temperature. In contrast, the spectra in the present compounds show features characteristic of the 'fast-relaxation' regime ($\nu \gg \nu_{hf}$): the magnetic splitting (or the hyperfine field) below T_N decreases as the transition is approached, which is indicative of fast fluctuations within the ground doublet. In the paramagnetic phase, the line splitting also decreases as temperature increases, which is indicative of fast interdoublet fluctuations. For these reasons, we think that the split spectra observed above T_N are pure quadrupolar hyperfine spectra, which implies that the Yb site symmetry is not cubic. A rough estimation of the exchange-driven (spin–spin) relaxation rate at low temperature yields $\nu_{ex} \sim k_B T_N/h \sim 20$ GHz, i.e. $\nu_{ex} \sim 300$ mm s^{-1}, meaning that the assumption of 'fast relaxation' is reasonable. Therefore, the line broadenings observed in the paramagnetic phase are mainly attributable to static effects; if one compares the mean square deviations $\sigma(\alpha_Q)$ measured in the magnetically ordered phase (0.5 mm s^{-1}) and in the paramagnetic phase (0.85 mm s^{-1}), one finds a reasonable agreement confirming our interpretation.

3.6. Low-temperature magnetic susceptibility measurements

The d.c. magnetic susceptibility of YbPdBi, measured down to 0.5 K in a field of 6.6 mT, is shown in figure 7, in units of emu cm^{-3}. A slope change is clearly seen at 1 K: in the temperature range 1 K $\leqslant T \leqslant$ 10 K, a Curie–Weiss law (1) is observed with $\mu_{eff} \simeq 3.7\ \mu_B$ and $\Theta_p \simeq 2$ K, while below 1 K, the slope of $\chi(T)$ increases drastically and the curvature changes sign. This singular point is certainly linked with the magnetic phase transition; however, it is neither typical of a ferromagnet, where $\chi(T)$ is expected to saturate below T_C towards the demagnetizing field limit $\chi(T_C) = 1/4\pi N$, nor of an antiferromagnet, for which a maximum in $\chi(T)$ is observed at T_N. Any demagnetizing field correction $4\pi N\chi$

would anyway be small with respect to unity in YbPdBi, as can be seen in figure 7.

The low-temperature Θ_p value of 2 K indicates the presence of antiferromagnetic interactions in YbPdBi, but the abrupt increase of the magnetic susceptibility below the magnetic transition temperature (1 K) could point to the presence of a small ferromagnetic component in the magnetic structure.

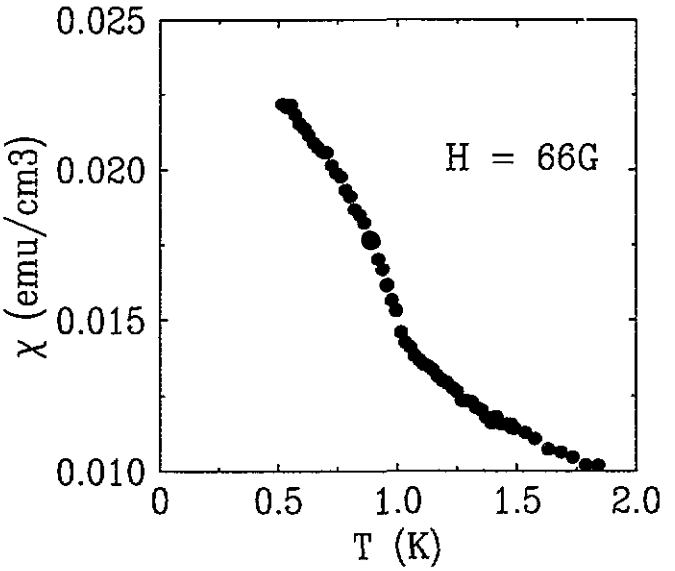

Figure 7. Low-temperature thermal variation of the magnetic susceptibility (in emu cm^{-3}) in YbPdBi.

4. The experimental results in YbNiSb

4.1. X-ray characterization

The x-ray diffraction pattern of our YbNiSb sample shows the lines of the f.c.c. lattice of the YbNiSb phase, and no impurity phase. The lattice parameter at room temperature is $a = 6.24225(5)$ Å. As in YbPdBi, the line intensities are close to those expected when the metal atom (Ni) lies at the (0, 0, 0) position. The precision on the line intensity measurements is, however, not sufficient to assess the presence of crystallographic order between the Yb and Sb sublattices.

Previous magnetic susceptibility measurements [11] show the presence of Yb^{3+} ions: $\chi(T)$ follows a Curie–Weiss law down to 25 K, with $\mu_{eff} \simeq 4.6\ \mu_B$, close to the free-ion value 4.54 μ_B, and a paramagnetic Curie temperature $\Theta_p \simeq 13$ K.

4.2. ^{170}Yb Mössbauer spectroscopy data

The Mössbauer data in YbNiSb are qualitatively similar to those in YbPdBi, although quantitatively somewhat different.

Above $T = 1$ K, the spectra are three-line hyperfine quadrupolar spectra (see figure 8, lower part), characteristic of the paramagnetic phase. This indicates that, as in YbPdBi, the Yb site symmetry is not cubic and that the spectra can be fitted to Hamiltonian (3), with an asymmetry parameter η close to unity. At $T = 1.4$ K, for instance, the fitted

Gaussian distribution of quadrupolar coupling parameters has the following characteristics: $\alpha_Q^0 = 2.1(1)$ mm s^{-1}, $\sigma(\alpha_Q) = 0.75$ mm s^{-1} and $\eta = 0.86$. The thermal variation of α_Q^0 is represented in figure 4; as temperature increases, it falls off more rapidly than in YbPdBi, showing that the first excited CEF level is closer to the ground state than in YbPdBi.

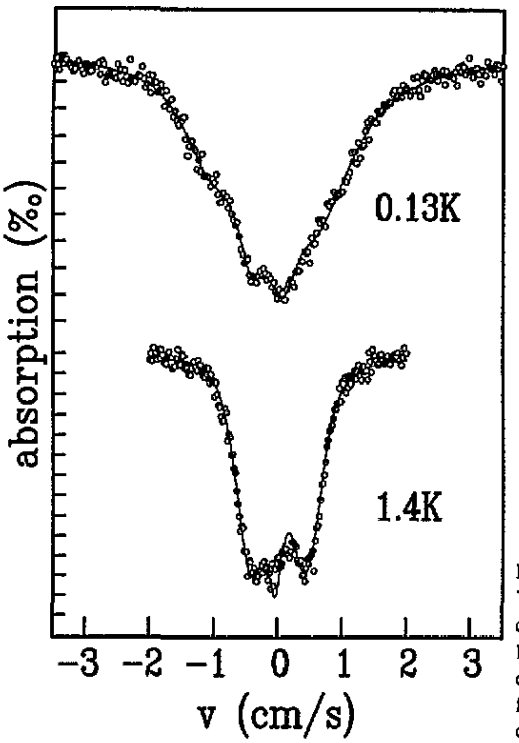

Figure 8. ^{170}Yb Mössbauer absorption spectra in YbNiSb in zero field at $T = 0.13$ K and 1.4 K. The continuous line for the 0.13 K spectrum is a fit to Hamiltonian (4) with Lorentzian-shaped lines having different linewidths; for the 1.4 K spectrum, it is a fit to Hamiltonian (3) with a Gaussian distribution of quadrupolar coupling parameter values.

Between 0.13 K and 0.85 K, the spectra show the presence of a hyperfine field, the linewidths being large and inhomogeneous. As in YbPdBi, this shows the presence of correlated distribution of hyperfine fields and quadrupolar parameters. However, an attempt to fit the $T = 0.13$ K spectrum using a linear correlation between H_{hf} and α_Q values failed, indicating that the root mean square deviation of the distribution of CEF energies is not small with respect to the energy of the first excited CEF level. This will be confirmed by the analysis in section 5.1.

At 0.13 K, the saturated hyperfine field is $H_{hf} = 108(10)$ T, and its orientation with respect to the EFG principal axes $OXYZ$ is defined by $\theta = 90°$ and $\gamma \sim 35°$. The derived saturated Yb^{3+} magnetic moment is $m = 1.06(10)\ \mu_B$; its thermal variation is represented in figure 6. The mean-field curve for $S = \frac{1}{2}$, with $T_N = 0.85$ K, is seen to be higher than the experimental points. The magnetic transition temperature $T_N = 0.85$ K is in good agreement with that derived from the position of the specific heat peak [10].

5. Interpretation and discussion

5.1. The crystal electric field level scheme of the Yb^{3+} ion

As the quadrupolar hyperfine interaction in the paramagnetic phase of both compounds has no cubic character at low temperature, this implies that the point symmetry of the Yb site

is not cubic. Therefore, the CEF level scheme of the Yb^{3+} ion in YbPdBi and YbNiSb consists of four Kramers doublets instead of the cubic decomposition into two doublets (Γ_6 and Γ_7) and the Γ_8 quartet. The following quantities yield information about the CEF level scheme in rare earth compounds:

(i) the neutron inelastic scattering spectra, which provide a direct measurement of the CEF transition energies;

(ii) the electronic 4f contribution to the specific heat in the paramagnetic phase (Schottky anomaly);

(iii) the thermal variation of the EFG components, which are the sum of a temperature-independent lattice charge contribution and the 4f quadrupolar moment contribution. The latter is temperature dependent; for instance, the principal value $V_{ZZ}^{4f}(T)$ is proportional to the thermal average of the main component of the 4f quadrupolar tensor Q_{ij}:

$$Q_{ZZ}(T) = \frac{1}{\mathcal{Z}} \sum_{i=1}^{4} Q_{ZZ}^{i} \exp\left(-\frac{\Delta_i}{k_B T}\right) \tag{5}$$

where $\mathcal{Z}$ is the partition function, and the quantities Q_{ZZ}^{i} and Δ_i are respectively the quantum mean value of the Z component of the 4f quadrupolar moment $3J_Z^2 - J(J+1)$ and the energy of the ith CEF Kramers doublet. In terms of the quadrupolar coupling parameter, the proportionality holds: α_Q^{4f} (mm s^{-1}) $= 0.276 Q_{ZZ}$.

In YbPdBi, the inelastic neutron scattering spectrum [13] at $T = 5$ K shows a peak at a transfer energy 7.5 meV, corresponding to a transition from the ground CEF doublet to an excited state (or towards two quasidegenerate states), and a rather broad low-energy structure centred around 2 meV. The thermal variation of the quadrupolar coupling parameter is very sensitive to the presence of a low-lying CEF state. Assuming that the lattice charge contribution is small, $\alpha_Q^0(T)$ was fitted to expression (5), with the help of the Laplace relation:

$$\sum_i Q_{ZZ}^{i} = 0. \tag{6}$$

We find that the observed decrease of $\alpha_Q(T)$ as temperature increases implies an energy $\Delta_2 \simeq 23$ K for the first CEF excited state, assuming either the presence of one doublet, or of two closely spaced doublets, around an energy 87 K (7.5 meV). Finally, the comparison of the experimental thermal variation of the 4f specific heat with Schottky anomalies due to such level schemes favours the scheme with one CEF state at about 20 K and two quasidegenerate states around 85 K. The dashed lines in figure 2 and in figure 4 represent respectively the Schottky anomaly and the calculated $\alpha_Q^0(T)$ using expression (5), with four Kramers doublets at energies 0, 23, 80 and 90 K. The $\alpha_Q^0(T)$ thermal variation and the low-temperature neutron inelastic spectrum are reasonably well reproduced by such a level scheme. For the specific heat, only qualitative agreement is achieved (figure 2); although the gross features of the $C_{4f}(T)$ variation can be described by means of this Schottky anomaly, one notes an enhanced contribution (~ 1 J K^{-1} mol^{-1}) near 10 K, for which we have at present no explanation. The weak Kondo coupling on the Yb^{3+} ion, suggested by the low-temperature specific heat data (see 5.3), does not seem to be responsible for this extra contribution to the specific heat, because the associated Kondo temperature T_K would be of the order of a few 10 K, and the presence of magnetic ordering in YbPdBi would then be highly unlikely. It is to be noted that no CEF level scheme can fully account for the thermal variation of the 4f electronic specific heat in YbPdBi.

In YbNiSb, the inelastic neutron scattering spectra at $T = 12$ K [14] show two peaks that can be attributed to CEF transitions from the ground doublet(s): one at an energy 6.2 meV, and another at an energy 17 meV. Assuming therefore that the two highest CEF doublets lie at energies 72 K (6.2 meV) and 200 K (17 meV), the thermal variation of $\alpha_Q^0(T)$ is well reproduced with the first excited CEF doublet at an energy $\Delta_2 \simeq 9$ K (dashed line in figure 4). As concerns the specific heat, this would lead to a low-temperature Schottky peak with an amplitude of 3.6 J K^{-1} mol^{-1} at $T \simeq 4$ K, in contradiction with the data of [10], which show that the zero-field specific heat in YbNiSb is constant, at a value 2 J K^{-1} mol^{-1}, in the temperature range 2 K–9 K (figure 3 in [10]). In order to solve this contradiction, we propose the following model: there is a sizeable distribution of crystal field distortions in YbNiSb, which leads to the distribution of hyperfine parameters observed in the Mössbauer spectra, and to a distribution of CEF energies. As the point symmetry of the Yb site is not known, the number and the values of the CEF parameters cannot be determined. Therefore, we simulate the CEF energy distribution by two independent Gaussian distributions for the energies of the two lowest Kramers doublets, with the same mean square deviation σ. The energies of the two highest Kramers doublets are not taken to be distributed, because they play a negligible role as concerns the low-temperature Schottky anomaly. We have also simulated the effect of a magnetic field by allowing a Zeeman splitting of the CEF states, each level being assigned a g factor equal to two, hence neglecting the crystalline anisotropy implied by the low Yb site symmetry. The mixing of the CEF wavefunctions by the magnetic field, which is especially important at high fields, is not taken into account. The results of the calculation of the low-temperature Schottky anomaly in zero field and in fields of 2.5T and 5.3T, together with the experimental data for the 4f specific heat in YbNiSb (after subtraction of the LuNiSb specific heat), are shown in figure 9. The theoretical curves were obtained with mean CEF energies 0, 9 K, 72 K and 200 K, and a mean square deviation $\sigma = 7$ K for the CEF energy distribution of the two lowest levels. This model, in spite of its crudeness, reproduces correctly the main features of the zero-field and low-field specific heat in YbNiSb below 20 K, in particular the constant level of 2 J K^{-1} mol^{-1} in zero field between 2 K and 9 K. At high fields, agreement is less satisfactory.

Such a distribution of CEF energies is certainly also present in YbPdBi, but it does not have the same drastic effect on the low-temperature Schottky anomaly as in YbNiSb because the first excited CEF level is higher in energy. We have indeed checked that a distribution of CEF energies cannot account for the observed discrepancy between the calculated and experimental specific heat.

5.2. Origin of the local symmetry breaking

The occurrence of a non-cubic Yb site symmetry at low temperature in a compound showing an x-ray diffractogram, at room temperature, characteristic of a cubic f.c.c. lattice raises the question of the presence of a crystallographic or quadrupolar phase transition below room temperature, or of strong atomic disorder.

To check for the presence of a phase transition, an x-ray diffractogram was measured at 20 K, and neutron diffraction spectra were recorded at 130 K and 1.5 K, in YbPdBi. The results show that there is no detectable modification of the diffraction spectra, by either technique, between high and low temperature, except for thermal expansion effects. The YbPdBi lattice appears therefore to be f.c.c. cubic down to 1.5 K. As to a phase transition due to the ordering of the 4f quadrupolar moments, which can occur with a very small and hence hardly detectable lattice distortion, its occurrence can be discarded in YbPdBi, between 1 K and 45 K, by the lack of any peak in the specific heat thermal variation.

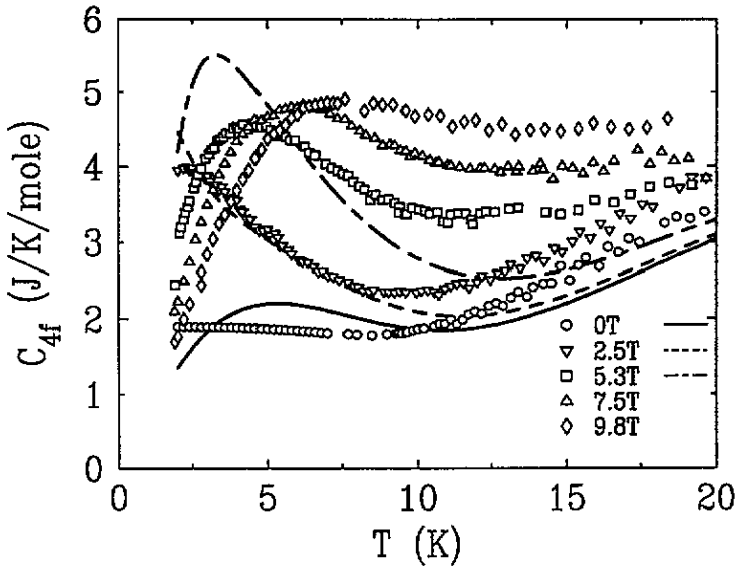

Figure 9. Temperature and field variation of the electronic 4f specific heat in YbNiSb below 20 K. The lines represent the calculated Schottky anomalies in fields of 0, 2.5 and 5.3 T according to the CEF model described in the text.

The presence of atomic disorder is more difficult to detect. The closeness of the electronic diffusion factors for Yb^{3+} ($Z = 67$), Sb ($Z = 51$) and Bi ($Z = 83$) precludes the use of the x-ray line intensities to detect atomic disorder between the Yb and Bi sublattices in YbPdBi, and between the Yb and Sb sublattices in YbNiSb. The neutron diffraction line intensities in the YbPdBi spectra cannot be measured with sufficient accuracy for this purpose. However, as the nearest neighbours of a Yb^{3+} ion are four metal atoms (Pd or Ni) on the vertices of a regular tetrahedron, disorder between Yb and the pnictogen atom alters only the next-nearest-neighbour environment of the Yb^{3+} ion, and must therefore have a limited influence, in a metallic compound, on the CEF symmetry at the Yb site. Actually, we think that an eventual Yb–pnictogen disorder can account for the observed distributions of distortions in both compounds, but not for the strong symmetry breaking at the Yb site. In this respect, it is of interest to note that an isostructural phase transition at $T = 100$ K has been suggested to occur in ZrNiSn, which crystallizes in the same MgAgAs-type structure [15]. This phase transition, evidenced by an anomaly in the thermal variation of the lattice parameter without any change in the crystal structure, is tentatively assigned by the authors to a spontaneous change of substitution degree between the Zr and Sn sublattices.

Without disregarding the possibility of an isostructural phase transition in YbPdBi and YbNiSb, we think, however, that the symmetry breaking is of local character, and our hypothesis is that it is due to a static Jahn–Teller effect within the Γ_8 cubic quartet. Among the cubic CEF eigenstates of a Kramers ion, the Γ_8 quartet alone, consisting of two degenerate Kramers doublets, can give rise to a Jahn–Teller effect, i.e. to a symmetry lowering leading to an energy gain. The Jahn–Teller effect would imply a static distortion of the YbM_4 'molecule', where M is Pd or Ni, which, in the studied compounds, would lift the degeneracy of the ground Γ_8 quartet and lead to a low-symmetry 4f quadrupolar tensor $\tilde{Q}_{ij}$ of the Yb^{3+} ion with the characteristics $Q_{ZZ} \simeq -Q_{XX}$, $Q_{YY} \simeq 0$, i.e. with an asymmetry parameter η close to unity. Such a value for η has already been encountered in Yb compounds where the symmetry of the Yb site is very low: in YbCuAl, which

crystallizes into a hexagonal lattice (space group $P\bar{6}2m$) and where the symmetry elements at the Yb site are two perpendicular mirrors [16], and in Yb_3Pd_4, which crystallizes into a rhombohedral lattice (space group $R3$) and where the Yb site possesses no symmetry elements [17].

The present explanation relies on the hypothesis that the Γ_8 quartet is the CEF ground state of the Yb^{3+} ion in an undistorted environment in this same lattice type, and it is supported by the study of the isostructural compound YbPdSb. In YbPdSb, ^{170}Yb Mössbauer spectroscopy and specific heat measurements [1–3] have been interpreted in terms of the Kondo effect on a Γ_8 CEF ground state, with a Kondo temperature $T_K \simeq 7$ K. The low-temperature inelastic neutron spectra in YbPdSb [1, 18] are somewhat similar to those in YbPdBi, showing an inelastic line at 6.5 meV. The ^{170}Yb Mössbauer spectra in YbPdSb above 1.4 K are one-line spectra, showing that the distortion of the Yb site, if any, is small and splits the Γ_8 ground state by no more than 1–2 K. Therefore, the occurrence of the Γ_8 quartet as the ground CEF state in these compounds is likely and, in YbPdBi and YbNiSb, a static Jahn–Teller effect could take place, splitting the Γ_8 quartet by ~ 10 K in YbNiSb and by ~ 20 K in YbPdBi, and leading to a Yb site with low symmetry. In cubic symmetry, the two Kramers doublets forming the Γ_8 quartet possess opposite quadrupole moments, corresponding to a quadrupolar hyperfine coupling parameter $\alpha_Q \simeq 2$ mm s^{-1}. In the 'fast-relaxation' regime of the paramagnetic phase, this yields a vanishing average EFG and therefore a single Mössbauer line. The intrinsic saturated magnetic moment of the Γ_8 quartet is anisotropic, but remains close to 2 μ_B. In the presence of a Jahn–Teller distortion, the Γ_8 character of the ground wavefunction is lost and, as the exact Yb site symmetry is not known, it is not possible to derive it starting from the measured quantities. It can be noticed that the α_Q saturated values in YbPdBi (2.85 mm s^{-1}) and in YbNiSb (2.1 mm s^{-1}) are close to that intrinsic to the Γ_8 quartet, and that the saturated magnetic moment of 1.25 μ_B in YbPdBi and of 1 μ_B in YbNiSb is smaller than the saturated Γ_8 moment.

As to the nature of this low-symmetry Yb site, we think that a small displacement of the Yb ion off its standard $(\frac{1}{4}, \frac{1}{4}, \frac{1}{4})$ special position in the cubic cell can be put forward: this would maintain a cubic f.c.c. lattice, with x-ray and neutron line intensities close to the standard ones, while drastically lowering the Yb site symmetry. The accuracy on the line intensity measurements in our powder diffraction experiments does not allow such a positional displacement to be detected.

5.3. The Kondo coupling on the Yb^{3+} ion

The presence of a weak Kondo coupling on the Yb^{3+} ion in an intermetallic compound showing magnetic ordering is most readily detected through the reduction of the entropy gain at the magnetic transition [19], which shows that the ionic spin degrees of freedom of the ground state are not completely released at the onset of the paramagnetic phase [20]. In YbPdBi, the entropy gain $R \ln 2$ expected for a Kramers doublet ground state is reached at a temperature $\sim 5T_N$, its value at T_N being only 40% of $R \ln 2$. The reduction of the specific heat peak value at the magnetic transition partly reflects this reduced entropy gain, but it is also due to the spread of the magnetic transition temperatures linked to the distribution of CEF parameters. The constant value 2.2 J K^{-1} mol^{-1} of the 4f-derived specific heat above T_N up to 3 K could be assigned to the tail of the Kondo anomaly on the doublet ground state, which has the form of a broad peak with amplitude 1.5 J K^{-1} mol^{-1} [21]. The associated Kondo temperature is certainly small, of the order of 1 K. The presence of Kondo coupling in YbNiSb is less clear, the entropy gain at the magnetic transition (0.85 K)

being $0.75R \ln 2$, close to the expected $R \ln 2$ value [10].

The Kondo coupling leads to a reduction of the spontaneous magnetic moment of the Yb ion with respect to its CEF-derived value [22]. In the case of YbPdBi, the saturated spontaneous Yb^{3+} magnetic moment was measured (1.25 μ_B), but an eventual reduction cannot be evidenced as the CEF parameters determining the ground state wavefunction are not known due to the symmetry lowering.

6. Conclusion

The ^{170}Yb Mössbauer absorption spectroscopy data obtained in the cubic alloys YbPdBi and YbNiSb in the temperature range 0.1 K–50 K show the presence of a second-order magnetic ordering transition at 1 K in YbPdBi, with a saturated Yb^{3+} magnetic moment of 1.25 μ_B, and confirm the presence of magnetic ordering below 0.85 K in YbNiSb, the saturated Yb^{3+} moment being 1.05 μ_B in this latter compound. In the paramagnetic phase, the spectra show that the symmetry of the Yb site is not cubic in either compound, and that the electric field gradient tensor at the Yb site has a quadrupolar asymmetry parameter close to unity, characteristic of a very low local symmetry. The thermal variation of the main component of the electric field gradient tensor shows that the first excited crystal electric field doublet has an energy of ~ 20 K in YbPdBi and of ~ 10 K in YbNiSb.

The 4f-derived electronic specific heat has been determined in YbPdBi in the temperature range 0.5 K–45 K. The analysis of the specific heat anomaly linked with the magnetic transition suggests the presence of a weak Kondo effect for the Yb^{3+} ion, and the main contribution to the high-temperature data is shown to be due to a crystal electric field Schottky anomaly. In YbNiSb, we present a simplified model, based on a distribution of crystal field parameters, which accounts for the main features of the field dependence of the electronic specific heat below 20 K.

Low-temperature x-ray and neutron diffraction spectra measured in YbPdBi show that there is no detectable lattice distortion in this compound down to 1.5 K. The non-cubicity of the Yb site symmetry is tentatively explained in terms of a local static Jahn–Teller effect that would split the Γ_8 quartet crystal electric field ground state by 10 K in YbNiSb and 20 K in YbPdBi.

Acknowledgment

We thank Professor K A Gschneidner Jr for making available to us the YbNiSb and LuNiSb samples and for helpful discussions.

References

[1] LeBras G 1994 *Thesis* Orsay

[2] LeBras G, Bonville P, Imbert P, Polatsek G, Besnus M J, Haen P and Moshchalkov V 1994 *Physica* B **199–200** 542

[3] LeBras G, Bonville P, Besnus M J, Haen P, Imbert P, Polatsek G and Aliev F G 1994 *Proc. Int. Conf. on Strongly Correlated Electronic Systems (Amsterdam, 1994)*

[4] Suzuki H, Kasaya M, Kohgi M, Dönni A, Fischer P, LeBras G and Bonville P 1994 *Proc. Int. Conf. on Strongly Correlated Electronic Systems (Amsterdam, 1994)*

[5] Fisk Z, Canfield P C, Beyermann W P, Thompson J D, Hundley M F, Ott H R, Felder E, Maple M B, Lopez de la Torre M A, Visani P and Seaman C L 1991 *Phys. Rev. Lett.* **67** 3310

[6] Amato A, Canfield P C, Feyerherm R, Fisk Z, Gygax F N, Heffner R H, MacLaughlin D E, Ott H R, Schenk A and Thompson J D 1992 *Phys. Rev.* B **46** 3151

[7] Canfield P C *et al* 1994 *Physica* B **197** 101
[8] Dhar S K, Nambudripad N and Vijayaraghavan R 1988 *J. Phys. F: Met. Phys.* **18** L41
[9] Aliev F G, Pak G I and Shkatova T M 1989 *Sov. Phys.–Solid State* **31** 1615
[10] Dhar S K, Ramakrishnan S, Vijayaraghavan R, Chandra G, Satoh K, Itoh J, Onuki Y and Gschneider K A Jr 1994 *Phys. Rev.* B **49** 641
[11] Dhar S K, Gschneider K A Jr, Vijayaraghavan R 1993 *Physica* B **186–188** 463
[12] Bonville P, Canaud B, Hammann J, Hodges J A, Imbert P, Jéhanno G, Severing A and Fisk Z 1992 *J. Physique* I **2** 459
[13] Marshall W G 1994 *Thesis* Oxford
[14] Adroja D T and Rainford B D 1994 *ISIS Experimental Report* vol II, p A66
[15] Aliev F G, Brandt N B, Moshchalkov V V, Kozyrkov V V, Skolozdra R V and Belogorokhov A I 1989 *Z. Phys.* B **75** 167
[16] Bonville P and Hodges J A 1985 *J. Magn. Magn. Mater.* **47&48** 152
[17] Bonville P, Hodges J A, Imbert P, Jéhanno G and Thuéry P 1994 *J. Magn. Magn. Mater.* **136** 238
[18] Dönni A, Fischer P, Kohgi M, Kasaya M 1993 *PSI Annual Report* p 66
[19] Besnus M J, Braghta A, Hamdaoui N and Meyer A 1992 *J. Magn. Magn. Mater.* **104–107** 1385
[20] A reduced entropy variation at the magnetic transition can also arise when the magnetic structure has an incommensurate character. See Bouvier M, Lethuillier P and Schmitt D 1991 *Phys. Rev.* B **43** 13 137
Blanco J A, Gignoux D and Schmitt D 1991 *Phys. Rev.* B **43** 13 145
[21] Rajan V T 1983 *Phys. Rev. Lett.* **51** 308
[22] Doniach S 1977 *Physica* B **91** 231